RAA 2021 Vol. **21** No. **7**, 180(7pp) doi: 10.1088/1674-4527/21/7/180

http://www.raa-journal.org *http://iopscience.iop.org/raa*

***R**esearch in*
***A**stronomy and*
***A**strophysics*

The deep and low-mass-ratio contact binary CSS J022914.4+044340 with a luminous additional companion

Liang Liu and Xu-Zhi Li

Yunnan Observatories, Chinese Academy of Sciences, Kunming 650216, China; *LiuL@ynao.ac.cn*
Key Laboratory for the Structure and Evolution of Celestial Objects, Chinese Academy of Sciences, Kunming 650216, China
Center for Astronomical Mega-Science, Chinese Academy of Sciences, Beijing 100101, China
University of Chinese Academy of Sciences, Beijing 100049, China

Received 2021 January 27; accepted 2021 March 12

Abstract The first B-, V-, R_c- and I_c-band light curves of CSS J022914.4+044340 are presented and analyzed. It is found that CSS J022914.4+044340 is a low mass ratio (0.198 ± 0.005) deep (63.7 ± 7.9 %) contact binary, indicating that it is already at the end evolutionary stage of tidally-locked evolution via magnetized wind. Because of the totally eclipsing character, the photometric solutions are reliable. The temperature and metallicity are determined from the spectroscopic data as $T = 5855 \pm 15$ K and [Fe/H] $= -0.842 \pm 0.031$, respectively. Based on the parallax of *Gaia* EDR3, the physical parameters of CSS J022914.4+044340 are estimated as $M_1 = 1.44^{+0.25}_{-0.22}\,M_\odot$, $M_2 = 0.29^{+0.05}_{-0.05}\,M_\odot$, $R_1 = 1.26^{+0.08}_{-0.06}\,R_\odot$, $R_2 = 0.65^{+0.03}_{-0.04}\,R_\odot$, $L_1 = 1.718^{+0.186}_{-0.191}\,L_\odot$ and $L_2 = 0.416^{+0.039}_{-0.050}\,L_\odot$. Combining the fraction of light from the third body via the photometric solution (54%), the luminosity of the third body is estimated as $2.705\,L_\odot$. The third body may be inferred to be a subgiant. Thus, why the primary component of CSS J022914.4+044340 has higher mass compared to similar systems is explained, as well as why its metallicity is so poor.

Key words: binaries : eclipsing — binaries : close — stars: individuals (CSS J022914.4+044340) — stars: evolution

1 INTRODUCTION

A contact binary is a close binary system whose components overflow their respective Roche lobes (Kopal 1959) and share a common envelope (CE). The CE is radiative if the system consists of O, B or maybe A spectral type stars, or else it is convective if the system is composed of later spectral type stars. Lucy (1968a,b) put forward a widely accepted convective common envelope (CCE) model for the W UMa-type contact binaries which contains two unevolved low mass components. Because of the tight orbit, contact binaries have the shortest periods, the lowest angular momenta and the strongest interactions among close binaries. They are very important for studying the processes of free mass and energy transfer, the interaction of components and characteristics of the CE. Due to the rapidly rotating later-type component, contact binaries usually display magnetic activities. In these cases, the light curves would be distorted by dark spots, the so-called O'Connell effect (O'Connell 1951). For some of them, the dark spots were found to change on a short timescale (e.g., GN Boo, Wang et al. 2015; V789 Her, Li et al. 2018). More importantly, contact binaries were associated with some special celestial systems. The progenitor of the luminous red nova (LRN) V1309 Sco (e.g., Tylenda et al. 2011; Stępień 2011) would be a deep and low-mass-ratio contact binary (DLMRCB) (Zhu et al. 2016). The Am-eclipsing binary V2787 Ori is also a shallow contact and extreme mass ratio contact binary (Tian et al. 2019). V53, a member of the globular cluster M4, could be a blue straggler (BS) (Li et al. 2017), and recently, Ferreira et al. (2019) reported that the post-burst V1309 Sco, a merger from a contact binary, is located in the BS region.

There is a period cutoff for contact binaries. This phenomenon was discovered by Rucinski (1992). According to the data at that time, he found the value of the period cutoff is about 0.22 d and he suggested that the limitation could be due to the fully convective structure of the

Table 1 New Times of Light Minima for CSS J022914.4+044340 with the 85 cm Telescope at Xinglong Station

HJD	Error (d)	Min	Filter
2458053.18427	0.00092	p	B
2458053.18284	0.00132	p	V
2458053.18365	0.00064	p	R_C
2458053.18401	0.00115	p	I_C
2458055.17658	0.00048	s	B
2458055.17673	0.00044	s	V
2458055.17663	0.00044	s	R_C
2458055.17565	0.00044	s	I_C

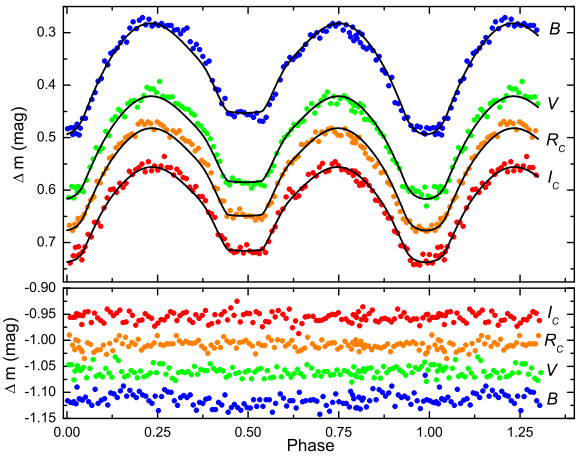

Fig. 1 In the upper panel, the *colored solid circles* refer to the observed differential light curves for CSS J022914.4+044340, while the *black solid lines* signify the theoretical light curves. Different colors denote different filters. The I_c-band light curve is shifted by $+0.05$ mag. The light curves in the lower panel correspond to the comparison star minus the check star (C-Ch). The symbols are the same as those in the upper panel.

M-type component. Later, Stępień (2006) explained this period limit as the shorter period detached binaries have not evolved into contact binaries within the age of the Universe, yet. Li et al. (2019) collected 55 such samples and suggested that in some cases, the effect of the third body should be taken into account except for those two reasons. They also suggested a statistical value for the period cutoff as 0.1763835 d. Very recently, Zhang & Qian (2020) suggested this value as 0.15 d. More information about the short period cutoff of contact binaries can be found in the review Qian et al. (2020, and the references therein).

Contact binaries are usually formed from detached binaries (e.g., Eggleton 2012) via angular momentum loss (AML) or via third bodies through the Kozai mechanism (Kozai 1962). According to the spectra provided by

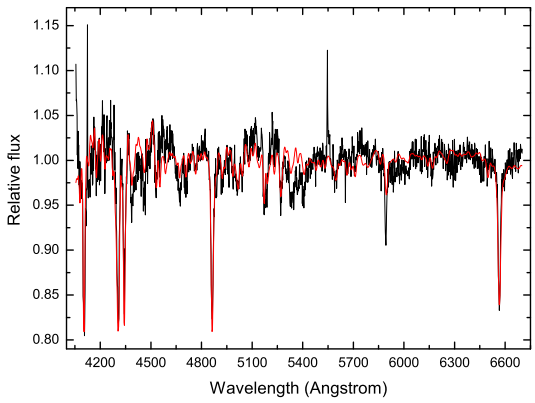

Fig. 2 Spectrum of CSS J022914.4+044340. The *black solid line* is the observed spectrum, while the *red solid line* is the fitting. The spectrum was observed by the 2.4-m telescope at Lijiang Gaomeigu Station, with Grism-14 and the $2.5''$ long-slit. The exposure time was 3600 s.

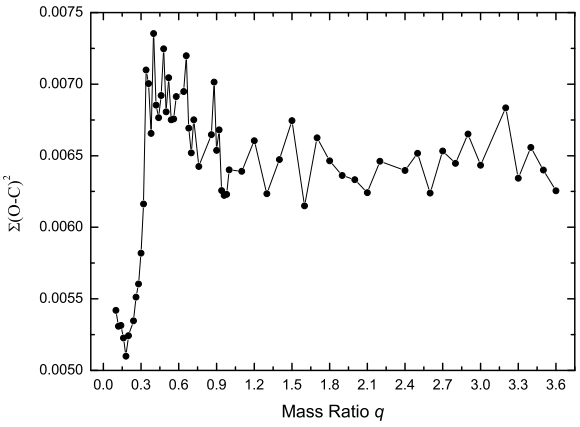

Fig. 3 The relation between q and the residual sum of squares for CSS J022914.4+044340. The optimally initial q is about 0.18.

LAMOST, Qian et al. (2017, 2018) found that EA-type binaries have higher metallicities than EW-type binaries and they suggest that long-period EWs should be formed by the EAs. During the contact evolutionary phase, there are at least two very important evolutionary stages for contact binaries, namely the marginal contact phase and the deep and low-mass-ratio (DLMR) contact phase (Qian et al. 2020). The marginal contact phase was predicted by thermal relaxation oscillation (TRO) theory (Lucy 1976; Flannery 1976; Robertson & Eggleton 1977). This theory assumes that matter can be transferred via the inner Lagrangian point while energy can be exchanged through the CCE. Mass transfer changes the

Table 2 Photometric Solutions for CSS J022914.4+044340

Parameters	Photometric elements	Errors
$g_1 = g_2$	0.32	assumed
$A_1 = A_2$	0.50	assumed
$x_{1\rm bol}, x_{2\rm bol}$	0.180,0.194	assumed
$y_{1\rm bol}, y_{2\rm bol}$	0.537,0.523	assumed
x_{1B}, x_{2B}	0.491,0.532	assumed
y_{1B}, y_{2B}	0.395,0.353	assumed
x_{1V}, x_{2V}	0.229,0.257	assumed
y_{1V}, y_{2V}	0.606,0.581	assumed
x_{1R_c}, x_{2R_c}	0.119,0.143	assumed
y_{1R_c}, y_{2R_c}	0.650,0.632	assumed
x_{1I_c}, x_{2I_c}	0.046,0.066	assumed
y_{1I_c}, y_{2I_c}	0.638,0.623	assumed
Phase shift	-0.0092	±0.0005
T_1 (K)	5855	±15
T_2 (K)	5747	±24
$q = M_2/M_1$	0.198	±0.005
$\Omega_{\rm in}$	2.2287	–
$\Omega_{\rm out}$	2.1021	–
$\Omega_1 = \Omega_2$	2.1480	±0.0099
$i(^\circ)$	88.4	±1.2
$L_1/(L_1+L_2)(B)$	0.8159	±0.0351
$L_1/(L_1+L_2)(V)$	0.8115	±0.0327
$L_1/(L_1+L_2)(R_c)$	0.8096	±0.0315
$L_1/(L_1+L_2)(I_c)$	0.8079	±0.0301
$l_3/(L_1+L_2+l_3)(B)$	0.5488	±0.0148
$l_3/(L_1+L_2+l_3)(V)$	0.5514	±0.0139
$l_3/(L_1+L_2+l_3)(R_c)$	0.5349	±0.0139
$l_3/(L_1+L_2+l_3)(I_c)$	0.5479	±0.0130
r_1(pole)	0.5073	±0.0027
r_1(side)	0.5595	±0.0042
r_2(back)	0.5887	±0.0057
r_2(pole)	0.2549	±0.0075
r_2(side)	0.2687	±0.0095
r_2(back)	0.3311	±0.0289
f (%)	63.7	±7.9

Table 3 Estimated Physical Parameters of CSS J022914.4+044340, Based on the Resolution and Parallax from *Gaia* EDR3

Parameters	Value	Range
T_1 (K)	5855	5840 ∼ 5870
T_2 (K)	5747	5723 ∼ 5771
M_1 $(M_\odot)$	1.44	1.22 ∼ 1.69
M_2 $(M_\odot)$	0.29	0.24 ∼ 0.34
R_1 $(R_\odot)$	1.26	1.20 ∼ 1.34
R_2 $(R_\odot)$	0.65	0.61 ∼ 0.68
L_1 $(L_\odot)$	1.718	1.527 ∼ 1.904
L_2 $(L_\odot)$	0.416	0.366 ∼ 0.455
A $(R_\odot)$	2.289	2.166 ∼ 2.418
$\log g_1$	4.39	4.37 ∼ 4.42
$\log g_2$	4.27	4.25 ∼ 4.29
$M_{\rm bol1}$	4.22	4.10 ∼ 4.34
$M_{\rm bol2}$	5.75	5.63 ∼ 5.87
m_V	14.255	14.204 ∼ 14.306
Distance (pc)	1600.0	1548.0 ∼ 1655.6
$(m-M)_V$	11.021	10.949 ∼ 11.095
BC_V	-0.121	$-0.171 \sim -0.071$
$M_{\rm bol}$	3.982	3.863 ∼ 4.102

The value of $M_{\rm bol}$ does not include the third light.

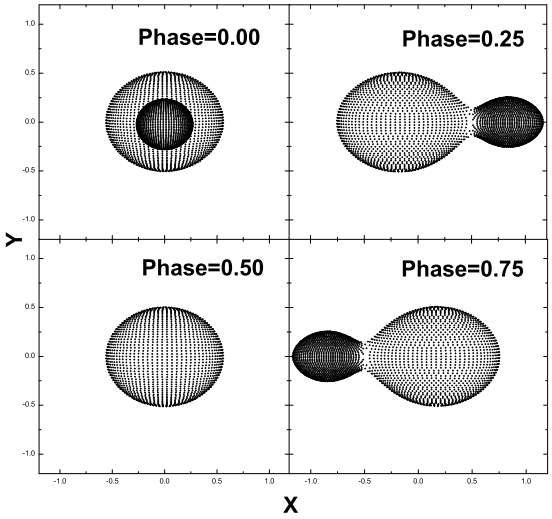

Fig. 4 The geometric structure of CSS J022914.4+044340 in different phases. It is obviously a totally eclipsing contact binary system.

orbit and energy transfer varies the surface temperature. Such processes make contact binaries oscillate between the semi-detached phase and the shallow contact phase. If the marginal contact binary has an appropriate rate of AML so that it counteracts the increased orbit caused by mass transfer, the system can stay in the zero-age and shallow contact phase (e.g., Rahunen 1981). Based on investigations of the period variations, it is suggested that contact systems can oscillate around a critical mass ratio on thermal timescales (e.g. $q_{\rm crit} = 0.4$, Qian 2001, 2003). Having undergone many such oscillations, contact binaries will evolve into the DLMR contact phase because of the increased rate of AML. A contact binary that has mass ratio $q \leqslant 0.25$ and fill-out factor $f \geqslant 50\%$ is suggested to be called a DLMRCB (e.g., Qian et al. 2005, 2006; Yang & Qian 2015). DLMRCBs are believed to merge into fast rotating single stars like FK Com-type stars or BSs because of dynamical instability caused by the extreme mass ratio or by the great depth of contact (e.g., Eggleton & Kiseleva-Eggleton 2001; Eggleton 2012).

CSS J022914.4+044340 (CRTS J022914.4+044340) was found to be an EW-type eclipsing binary by Drake et al. (2014). It was taken as a candidate of DLMRCB because of the flat bottom profile on its minimum and low amplitude of its light variations. This target was observed by LAMOST several times. According to the latest data release of LAMOST (Luo et al. 2019), we have $T = 5767.91 \pm 85.13$ K and [Fe/H]$= -0.922 \pm 0.082$. We can also find this target in the *Gaia* Data Release 2 (DR2) and *Gaia* Early Data Release 3 (EDR3). Then we have $T = 5864.25^{+260.41}_{-79.25}$ K, G $= 14.2893 \pm 0.0072$ mag (Gaia Collaboration et al. 2018) and parallax

$= 0.6250 \pm 0.0210$ mas (Gaia Collaboration 2020). This parallax corresponds to a distance of $1600.0^{+55.6}_{-52.0}$ pc. This paper is organized as follows. In Section 2, the photometric and spectroscopic observations for this target are introduced briefly. In Section 3, the light curve solution is obtained via the Wilson-Devinney (W-D) code. In Section 4, the physical parameters are estimated. The last section is about discussions and conclusion.

2 PHOTOMETRIC AND SPECTROSCOPIC OBSERVATIONS AND DATA REDUCTION

The B-, V-, R_c- and I_c-band light curves of CSS J022914.4+044340 were carried out in two nights on 2017 October 26 and 28, with an Andor DZ936 2K CCD camera attached to the 85 cm reflecting telescope at Xinglong Station of National Astronomical Observatories, Chinese Academy of Sciences. The observational system has a standard Johnson-Cousins-Bessel multi-color CCD photometric system attached at the primary focus (Zhou et al. 2009), generating an effective field of view equal to 33×33 arcmin^2. The integration times were 80 s for the B-band, 50 s for the V-band, 40 s for the R_c-band and 30 s for the I_c-band. During the observation, the weather was clear and the seeing was about $1.2''$.

To avoid cumbersome standard photometry, the differential photometry method was applied to measure the light curves of the variable star. The effect of atmospheric extinction can be easily eliminated with this method by selecting suitable comparison and check stars. In this reduction, 2MASS J02285932+0444322 and 2MASS J02290506+0441298 were chosen as comparison star and check star, respectively. According to the *Gaia* DR2 (Gaia Collaboration et al. 2018), we have $T = 5431.93$ K, G $= 13.7433$ mag for the comparison and $T = 5375.50$ K, G $= 14.7731$ mag for the check star. The observed data were reduced by IRAF, with the bias and flat corrections. PHOT was utilized to obtain the instrument magnitudes of the chosen stars. All frames are measured. The measuring errors of the magnitude (~ 0.02 mag) mainly come from the lower signal-to-noise ratio (S/N) because of the faint target. The phases of CSS J022914.4+044340 are calculated according to the ephemeris Min.I $= 2458055.17640 + 0^d.306139 \times E$. T_0 of 2458055.17640 fitted by a parabola with the least squares method is the primary minimum of this observation, and P_0 of $0^d.306139$ is from the study of Qian et al. (2017). One can find the corresponding light curves in Figure 1. Several new times of minima determined via the parabolic fitting method are listed in Table 1.

We determine the temperature of CSS J022914.4+044340 by using of the Yunnan Faint Object Spectrograph and Camera (YFOSC). The spectroscopic observations were carried out on 2020 January 17, with the 2.4-m telescope in Lijiang Gaomeigu Station. The filter is Grism-14 covering the wavelength from 320 to 750 nm, while the long-slit is about $2.5''$. More details on this spectroscopic system can be found in Fan et al. (2015). Because our target is faint, an exposure time of 3600 s was adopted. We employed IRAF to eliminate the effects of bias and flat field on the picture. Then, we utilized the APEXTRACT package to extract the spectra. The comparison spectra for wavelength calibration was from the He-Ne lamp. Finally, we fit the reduced spectrum with the package University of Lyon Spectroscopic analysis Software (ULySS) (Koleva et al. 2009; Wu et al. 2011). UlySS is a full-spectrum fitting method for the analysis of stellar atmospheric parameters and stellar population spectra. In this method, chi-square maps are examined to study the degeneracies; convergence maps are constructed to determine the local minima; and Monte Carlo simulations are relied on to estimate the errors. The observed spectrum of CSS J022914.4+044340 and the corresponding fitting are listed in Figure 2. According to this fitting, we obtain that $T_{\rm eff} = 5855 \pm 15$ K and [Fe/H] $= -0.842 \pm 0.031$.

3 LIGHT CURVE SOLUTION

To determine the photometric elements and further to understand the geometrical structure and evolutionary state of CSS J022914.4+044340, the latest version of the W-D code (Wilson & Devinney 1971; Wilson 1979, 1990, 2008, 2012; Van Hamme & Wilson 2007; Wilson et al. 2010; Wilson & Van Hamme 2014) is employed to analyze the multi-color light curves. The q-search method is adopted to find an initial value of q. The result of the q-search, which is shown in Figure 3, suggests an initial value of q to be 0.18.

The temperature of CSS J022914.4+044340 is about $T_{\rm eff} = 5855 \pm 15$ K, which suggests a convective equilibrium for this system, corresponding to a bolometric albedo of $A_1 = A_2 = 0.5$ (Rucinski 1969) and a gravity-darkening coefficient of $g_1 = g_2 = 0.32$ (Lucy 1967). We adopt the square root law to handle the effect of limb-darkening, because the given errors for this law on that temperature are the smallest. The values of the limb-darkening coefficients come from Claret & Bloemen (2011). The adjusted parameters are the mass ratio q, the mean temperature of star 2, T_2, the monochromatic luminosity of star 1 and the dimensionless potential of star 1 (mode 3, $\Omega_1 = \Omega_2$). The related limb-darkening coefficients vary with T_2. We also adjust l_3 according to the luminosity of the third body in the line of sight, finding that the third light is more than half the luminosity of the system. The solved photometric parameters are listed in

Table 4 DLMRCBs with q around 0.20

Star	Period (d)	q M_2/M_1	M_1 ($M_\odot$)	M_2 ($M_\odot$)	R_1 ($R_\odot$)	R_2 ($R_\odot$)	L_1 ($L_\odot$)	L_2 ($L_\odot$)	f %	i (°)	T_1 (K)	T_2 (K)	Reference
TZ Boo	0.2971599	0.207	0.99	0.21	1.08	0.56	1.260	0.330	52.5	85.5	5890	5873	[1]
CSS J022914.4+044340	0.306139	0.198	1.44	0.29	1.26	0.65	1.718	0.416	63.7	88.2	5855	5744	[2]
BO Ari	0.3182	0.209	1.14	0.24	1.16	0.61	1.470	0.440	50.3	85.7	5920	6055	[3]
V1853 Ori	0.3830	0.203	1.23	0.25	1.38	0.71	2.490	0.690	50.0	83.2	6200	6261	[4]
NSVS 6859986	0.38356914	0.208	1.87	0.39	1.63	0.84	1.620	0.430	86.4	89.0	5100	5100	[5]
TYC 3836-0854-1	0.41556601	0.190	1.200	0.228	1.46	0.75	3.091	0.795	79.4	77.5	6332	6292	[6]
MQ UMa	0.47606620	0.195							82.0	65.6	6352	6224	[7]
DN Aur	0.6169	0.205	1.44	0.30	1.98	1.01	7.570	1.880	53.9	76.9	6830	6750	[8]
HV UMa	0.7108	0.190	2.84	0.54	2.62	1.18	17.220	2.950	61.9	57.3	7300	7000	[9]

Reference: [1] Christopoulou et al. (2011); [2] This paper; [3] Yang & Qian (2015); [4] Samec et al. (2011); [5] Kjurkchieva et al. (2019); [6] Liao et al. (2017); [7] Zhou et al. (2015); [8] Goderya et al. (1996); [9] Csák et al. (2000).

Table 2, while the fitted light curves are plotted in Figure 1. It is illustrated with Figure 1 that CSS J022914.4+044340 is a totally eclipsing binary.

4 PHYSICAL PARAMETER ESTIMATION

We have introduced how to estimate the absolute parameters (M, R, L) with errors via the parallax given by *Gaia* in a very recent paper (Liu et al. 2020). We know that the parallax of CSS J022914.4+044340 is 0.6250 ± 0.0210 mas (*Gaia* EDR3, Gaia Collaboration 2020), corresponding to a distance of $1600.0^{+55.6}_{-52.0}$ pc, yielding a modulus of $11.021^{+0.074}_{-0.072}$ mag. We also know the V-band magnitude to be 13.835 ± 0.051 mag (URAT1 Catalog, Zacharias et al. 2015) for our comparison star (2MASS J02285932+0444322). From the light curves (the upper panel of Fig. 1), we determine that the maximum V-band magnitude of CSS J022914.4+044340 is about 14.256 mag while the corresponding minimum magnitude is about 14.456 mag. Thus we infer the absolute magnitude to be $3.235^{+0.074}_{-0.072}$ mag in V-band at the phase of 0.25 or 0.75. According to Worthey & Lee (2011), we have a bolometric correction coefficient for V-band of -0.121 ± 0.050 mag under the conditions of $T = 5855 \pm 15$ K and [Fe/H] $= -0.842 \pm 0.031$. Therefore, we estimate the absolute bolometric magnitude of CSS J022914.4+044340 to be $3.114^{+0.124}_{-0.122}$ mag. By applying the formulae introduced in our paper that was published earlier this year (Liu et al. 2020), we have $M_1 = 1.44^{+0.25}_{-0.22}\,M_\odot$, $M_2 = 0.29^{+0.05}_{-0.05}\,M_\odot$, $R_1 = 1.26^{+0.08}_{-0.06}\,M_\odot$, $R_2 = 0.65^{+0.03}_{-0.04}\,M_\odot$, $L_1 = 1.718^{+0.186}_{-0.191}\,L_\odot$ and $L_2 = 0.416^{+0.039}_{-0.050}\,L_\odot$ for each component of CSS J022914.4+044340. These errors are derived from the error transfer formula. All estimated parameters are listed in Table 3.

5 DISCUSSION AND CONCLUSIONS

Based on the solution of multiple colored light curves and the analysis of their uncertainties, we found that CSS J022914.4+044340 is an extreme mass ratio (0.198 ± 0.005), deep contact binary ($63.7 \pm 7.9\%$). The 38-minute flat bottom in light curve, as well as the high inclination ($88.4° \pm 1.2°$), indicates a total eclipse of this binary system (as depicted in Fig. 4). The photometric solutions would be reliable if the system were totally eclipsing (Terrell & Wilson 2005). Based on that, the physical parameters have been estimated by its photometric solutions with its distance determined by *Gaia* EDR3. To avoid the potential error brought from the temperature (e.g., Liu et al. 2020), we have determined the temperature of CSS J022914.4+044340 through the spectroscopic data obtained by the YFOSC. The determined value is 5855 ± 15 K which is consistent with the value of 5767.91 ± 85.13 K provided by LAMOST Data Release 5 (DR5) (Luo et al. 2019) and of $5864.25^{+260.41}_{-79.25}$ K given by *Gaia* DR2 (Gaia Collaboration et al. 2018). Our derived value of metallicity of [Fe/H] $= -0.842 \pm 0.031$ is also similar to the value of -0.922 ± 0.082 supplied by LAMOST DR5 (Luo et al. 2019).

According to the statistics (Qian et al. 2017), the peak of metallicity for EW-type binaries is about -0.3. CSS J022914.4+044340 is close to the critical poorer metallicity boundary. This may be caused by a luminous third body. Our solved third body contributes over 54% of light in the system. Although it is very common that there is a third body in contact binaries (e.g., Pribulla & Rucinski 2006; D'Angelo et al. 2006; Rucinski et al. 2007), the luminous contribution of the third bodies being over 20% is little. About 23% of the luminosity in V345 Gem comes from the third body (Yang et al. 2009). These fractions are 25% for MQ UMa (Zhou et al. 2015), 28% for II UMa (Zhou et al. 2016) and 20% for TZ Boo (Christopoulou et al. 2011). Except for II UMa, the orbital periods of these targets showed cyclic variations which would be caused by the light-travel-time effect (LTTE) (e.g., Liao & Qian 2010). According to D'Angelo et al. (2006), II UMa contains a third body separated by 0.87″. Lack of the LTTE may be due to the long orbital period of the third body or it is a foreground/background star. The luminosity of

the third body in CSS J022914.4+044340 is about 54%. This fraction is very high. According to this fraction, the luminosity of this third body is estimated as $2.705\,L_{\odot}$, corresponding to a main-sequence star with a mass of $1.3\,M_{\odot}$ or a G5 subgiant with a mass of $1.1\,M_{\odot}$ (Cox 2000). If it were the former, its temperature as well as the metallicity would be a little higher than that of the Sun so that the corresponding values of CSS J022914.4+044340 should be lower than the derived valves mentioned above. The results would be reversed if it were the latter one. We also note that the mass of the primary is $M_1 = 1.44^{+0.25}_{-0.22}\,M_{\odot}$, but the temperature is 5855 ± 15 K. The observed temperature of CSS J022914.4+044340 may be lower because of the existence of the conjectured subgiant third body. For the same reason, the observed metallicity may be lower, too. Hence, the real metallicity of CSS J022914.4+044340 may be not as low as the value of [Fe/H] $= -0.842 \pm 0.031$. Whether the parallax was affected by the third body is not clear.

On the other hand, contact binaries are taken as distance tracers because of the period-color correlation first discovered by Eggen (1967). The absolute-magnitude calibration of contact binaries was developed by Rucinski (1994, 2000, 2004), via the parallax data of the *Hipparcos* mission (ESA 1997) and contact binaries in open or globular clusters. By using the first *Gaia* data release (Data Release 1, DR1; Gaia Collaboration et al. 2016a,b), Mateo & Rucinski (2017) improved this calibration. According to their formula

$$M_V = 3.73 - 8.67(\log P + 0.40)\,, \qquad (1)$$

substituting $P = 0.306139$ d, we have $M_V = 4.719$ mag for CSS J022914.4+044340. However, the M_V should be 4.103 mag after excluding the affect of the third light. This difference may be caused by bias in the temperature which was affected by the third light. DLMCBs with similar mass ratio as CSS J022914.4+044340 are collected in Table 4. It is seen that CSS J022914.4+044340 is very similar to TZ Boo which has a spectroscopic mass ratio. However, the mass of the primary component of the former one is much larger. Again, this should be on account of the affect of the third light.

Based on the above analysis, we conclude that CSS J022914.4+044340 is a DLMRCB. It contains a perhaps subgiant third companion with an inferred mass of $1.1\,M_{\odot}$. The presence of the third body makes the contact binary system seem cooler and metallicity poorer. The real mass of the primary component of CSS J022914.4+044340 should be a little less than $1.44\,M_{\odot}$.

Acknowledgements We are grateful to the anonymous referee who gave very useful suggestions that improved the paper. We acknowledge supports from the staff at the Xinglong 85-cm telescope and at the Lijiang 2.4-m telescope. We also acknowledge supports from the National Natural Science Foundation of China (Grant Nos. 11773066 and 11933008), from the CAS Interdisciplinary Innovation Team, from the Young Academic and Technology Leaders Project of Yunnan Province (No. 2015HB098), and from the Open Project Program of the Key Laboratory of Optical Astronomy, National Astronomical Observatories, Chinese Academy of Sciences.

References

1997, ESA Special Publication, 1200, The HIPPARCOS and TYCHO Catalogues, Astrometric and Photometric Star Catalogues Derived from the ESA HIPPARCOS Space Astrometry Mission

Christopoulou, P. E., Parageorgiou, A., & Chrysopoulos, I. 2011, AJ, 142, 99

Claret, A., & Bloemen, S. 2011, A&A, 529, A75

Cox, A. N. 2000, Allen's Astrophysical Quantities

Csák, B., Kiss, L. L., Vinkó, J., & Alfaro, E. J. 2000, A&A, 356, 603

D'Angelo, C., van Kerkwijk, M. H., & Rucinski, S. M. 2006, AJ, 132, 650

Drake, A. J., Graham, M. J., Djorgovski, S. G., et al. 2014, ApJS, 213, 9

Eggen, O. J. 1967, MmRAS, 70, 111

Eggleton, P. P. 2012, Journal of Astronomy and Space Sciences, 29, 145

Eggleton, P. P., & Kiseleva-Eggleton, L. 2001, ApJ, 562, 1012

Fan, Y.-F., Bai, J.-M., Zhang, J.-J., et al. 2015, RAA (Research in Astronomy and Astrophysics), 15, 918

Ferreira, T., Saito, R. K., Minniti, D., et al. 2019, MNRAS, 486, 1220

Flannery, B. P. 1976, ApJ, 205, 217

Gaia Collaboration 2020, VizieR Online Data Catalog: Gaia EDR3 (Gaia Collaboration, 2020), in VizieR Online Data Catalog, I/350

Gaia Collaboration, Brown, A. G. A., Vallenari, A., Prusti, T., & et al. 2016a, A&A, 595, A2

Gaia Collaboration, Brown, A. G. A., Vallenari, A., Prusti, T., & et al. 2018, A&A, 616, A1

Gaia Collaboration, Prusti, T., de Bruijne, J. H. J., Brown, A. G. A., & et al. 2016b, A&A, 595, A1

Goderya, S. N., Leung, K. C., & Schmidt, E. G. 1996, Ap&SS, 246, 291

Kjurkchieva, D. P., Popov, V. A., & Petrov, N. I. 2019, AJ, 158, 186

Koleva, M., Prugniel, P., Bouchard, A., & Wu, Y. 2009, A&A, 501, 1269

Kopal, Z. 1959, Close binary systems, (New York: Springer US)

Kozai, Y. 1962, AJ, 67, 591
Li, K., Hu, S., Chen, X., & Guo, D. 2017, PASJ, 69, 79
Li, K., Xia, Q. Q., Hu, S. M., Guo, D. F., & Chen, X. 2018, PASP, 130, 074201
Li, K., Xia, Q.-Q., Michel, R., et al. 2019, MNRAS, 485, 4588
Liao, W. P., & Qian, S. B. 2010, MNRAS, 405, 1930
Liao, W. P., Qian, S. B., Soonthornthum, B., et al. 2017, PASP, 129, 124204
Liu, L., Qian, S., Li, K., et al. 2020, Ap&SS, 365, 71
Lucy, L. B. 1967, ZAp, 65, 89
Lucy, L. B. 1968a, ApJ, 153, 877
Lucy, L. B. 1968b, ApJ, 151, 1123
Lucy, L. B. 1976, ApJ, 205, 208
Luo, A. L., Zhao, Y. H., Zhao, G., et al. 2019, VizieR Online Data Catalog, V/164
Mateo, N. M., & Rucinski, S. M. 2017, AJ, 154, 125
O'Connell, D. J. K. 1951, Publications of the Riverview College Observatory, 2, 85
Pribulla, T., & Rucinski, S. M. 2006, AJ, 131, 2986
Qian, S. 2001, MNRAS, 328, 635
Qian, S. 2003, MNRAS, 342, 1260
Qian, S.-B., He, J.-J., Zhang, J., et al. 2017, RAA (Research in Astronomy and Astrophysics), 17, 087
Qian, S. B., Yang, Y. G., Soonthornthum, B., et al. 2005, AJ, 130, 224
Qian, S. B., Zhang, J., He, J. J., et al. 2018, ApJS, 235, 5
Qian, S.-B., Zhu, L.-Y., Liu, L., et al. 2020, RAA (Research in Astronomy and Astrophysics), 20, 163
Qian, S., Yang, Y., Zhu, L., He, J., & Yuan, J. 2006, Ap&SS, 304, 25
Rahunen, T. 1981, A&A, 102, 81
Robertson, J. A., & Eggleton, P. P. 1977, MNRAS, 179, 359
Rucinski, S. M. 1969, AcA, 19, 245
Rucinski, S. M. 1992, AJ, 103, 960
Rucinski, S. M. 1994, PASP, 106, 462
Rucinski, S. M. 2000, AJ, 120, 319
Rucinski, S. M. 2004, New Astron. Rev., 48, 703
Rucinski, S. M., Pribulla, T., & van Kerkwijk, M. H. 2007, AJ, 134, 2353
Samec, R. G., Labadorf, C. M., Hawkins, N. C., Faulkner, D. R., & Van Hamme, W. 2011, AJ, 142, 117
Stępień, K. 2006, Acta Astronomica, 56, 347
Stępień, K. 2011, A&A, 531, A18
Terrell, D., & Wilson, R. E. 2005, Ap&SS, 296, 221
Tian, X.-m., Zhu, L.-y., & Wang, Z.-h. 2019, PASP, 131, 084203
Tylenda, R., Hajduk, M., Kamiński, T., et al. 2011, A&A, 528, A114
Van Hamme, W., & Wilson, R. E. 2007, ApJ, 661, 1129
Wang, J. J., Qian, S. B., Zhang, Y. P., et al. 2015, AJ, 149, 164
Wilson, R. E. 1979, ApJ, 234, 1054
Wilson, R. E. 1990, ApJ, 356, 613
Wilson, R. E. 2008, ApJ, 672, 575
Wilson, R. E. 2012, AJ, 144, 73
Wilson, R. E., & Devinney, E. J. 1971, ApJ, 166, 605
Wilson, R. E., & Van Hamme, W. 2014, ApJ, 780, 151
Wilson, R. E., Van Hamme, W., & Terrell, D. 2010, ApJ, 723, 1469
Worthey, G., & Lee, H.-c. 2011, ApJS, 193, 1
Wu, Y., Singh, H. P., Prugniel, P., Gupta, R., & Koleva, M. 2011, A&A, 525, A71
Yang, Y.-G., & Qian, S.-B. 2015, AJ, 150, 69
Yang, Y. G., Qian, S. B., Zhu, L. Y., & He, J. J. 2009, AJ, 138, 540
Zacharias, N., Finch, C., Subasavage, J., et al. 2015, AJ, 150, 101
Zhang, X.-D., & Qian, S.-B. 2020, MNRAS, 497, 3493
Zhou, A.-Y., Jiang, X.-J., Zhang, Y.-P., & Wei, J.-Y. 2009, RAA (Research in Astronomy and Astrophysics), 9, 349
Zhou, X., Qian, S. B., Liao, W. P., et al. 2015, AJ, 150, 83
Zhou, X., Qian, S. B., Zhang, J., et al. 2016, ApJ, 817, 133
Zhu, L.-Y., Zhao, E.-G., & Zhou, X. 2016, RAA (Research in Astronomy and Astrophysics), 16, 68